# ACTIVE STEERING OF RAILWAY VEHICLES: A FEEDFORWARD STRATEGY

**Shuiwen Shen*, TX Mei*, R.M.Goodall†, J.Pearson†, G.Himmelstein‡**

* University of Leeds LS2 9JT, Leeds UK. Tel:(40)113+3432064, email:s.shen@ee.leeds.ac.uk
† Department of E&E Eng, Loughborough University, LE11 3TU, Loughborough UK.
† Bombardier Transportation, Siegen, Germany.

**Keywords:** Active control, Vehicle dynamics, Steering, Sensitivity, Feedforward.

## Abstract

This paper presents an active steering strategies for a railway vehicle to improve performances on curves. By feeding forward a desired angle of attach and the radius of curves, a feedforward control law is proposed and verified. In order to assess its performance issue, parameter variations such as creep coefficients and nonlinearities of the wheel conicity are considered. The simulation results show a significant improvement. Although the feedforward strategy depends on the knowledge of the yaw stiffness of the system, no interference with the stability make it preferable.

## 1 Introduction

A well-known conflict between stability and steering for railway vehicles with coned/profiled wheels has been a challenge [1]. Though the kinematic instability of the solid-axle wheelsets can be removed through a stiff yaw connection, it deteriorates curving performances [2]. There have been many investigations on the possible mechanical solutions such as cross-bracing, body steering and primary yaw damping, by which the trade-off can be improved [3]. However the contradiction between high-speed stability and effective curving still remains. Active control can provide a solution for this problem, although so far the practical applications are restricted to the secondary suspension to improve ride quality. The incorporation of active control offers a design flexibility which is not available in any mechanical suspensions. With such a flexibility, a number of publications illustrate the possibility of removing the trade-off. In contrast to previous studies of active stability [4], active yaw relaxation [2] and active the lateral position and/or the yaw moment of the wheelset control [5], this paper investigates a feedforward strategy, which offers a practical solution for improving curvature performance without compromising the stability.

The remainder of this paper is organized as follows. In addition to a description of a railway vehicle, a brief introduction of an active strategy toward vehicle stability is presented in Section 2. Focusing on a comparison between so-called radial and perfect steering, the feedforward strategies are detailed in Section 3 and assessed in Section 4. Finally, Section 5 gives the main conclusions and some suggestions for future research.

## 2 Basic Principles

A plan view of a half-vehicle is depicted in Fig.1 (a), in which two actuators are located between wheelsets and the bogie frame. Appendices B and C present the necessary parameters and their normal quantities, respectively. An introduction of three reference coordinates provides a convenience of modeling the system, where the coordinate $FL$ is attached to and moving with the leading wheelset; the coordinate $FT$ is relevant to the trailing wheelset; and the coordinate $FG$ applies to the bogie frame and body. The three coordinates move with the same velocity $v_s$ as the longitudinal dynamics are not modeled. Each coordinate has its own yaw velocity of $\omega_l = -v_s/R_l$, $\omega_t = -v_s/R_t$ and $\omega_g = -v_s/R$ *w.r.t.* the track, but only one of them is independent since the frames are inter-related by the angles of $\phi_l = l_y/R_l$ and $\phi_t = l_y/R_t$. In addition, the equivalent yaw stiffness and damping of the primary suspensions are employed to represent their effect on the yaw dynamics of the wheelset and bogie. The equivalent yaw stiffness and damping *w.r.t.* the wheelsets are $K_{pw} = k_{px}\ l_y^2$, $B_{pw} = b_{px}\ l_y^2$ whereas, $K_{pg} = k_{px}\ l_y^2 + k_{py}\ l_x^2$ and $B_{pg} = b_{px}\ l_y^2 + b_{py}\ l_x^2$ are *w.r.t.* the bogie. The rail/wheel creep forces generally depend both on creepages, being relative normalised velocities between the rail and wheel, and the creep coefficients, depending on the vertical loads at individual wheels. Accordingly, the lateral creep forces of the wheelsets are given by

$$F_{yl} = -2\ f_{22}\ \left(\frac{\dot{y}_l}{v_s} - \psi_l\right) \quad (1)$$

$$F_{yt} = -2\ f_{22}\ \left(\frac{\dot{y}_t}{v_s} - \psi_t\right) \quad (2)$$

The torques at the wheelsets due to the longitudinal creepages are represented as follows.

$$T_l^{crp} = 2\ l_g\ f_{11}\ \left(\frac{y_l - y_{rl}}{r_0}\ \lambda - \frac{l_g}{R_l} + \frac{l_g\ \dot{\psi}_l}{v_s}\right) \quad (3)$$

$$T_t^{crp} = 2\ l_g\ f_{11}\ \left(\frac{y_t - y_{rt}}{r_0}\ \lambda - \frac{l_g}{R_t} + \frac{l_g\ \dot{\psi}_t}{v_s}\right) \quad (4)$$

By introducing $\chi_l = 1/R_l$, $\chi_t = 1/R_t$, $F_{11} = 2f_{11}$, and $F_{22} = 2f_{22}$, a state-space representation is expressed as

$$\dot{\mathbf{x}} = \mathbf{A}\ \mathbf{x} + \mathbf{B}\ \mathbf{u} + \mathbf{P}\ \mathbf{w} \quad (5)$$

where the states $\mathbf{x}$, inputs $\mathbf{u}$, and disturbances $\mathbf{w}$ are given by,

$$\mathbf{x} = \left[y_l,\ y_t,\ y_g,\ y_b,\ \psi_l,\ \psi_t,\ \psi_g,\ \dot{y}_l,\ \dot{y}_t,\ \dot{y}_g,\ \dot{y}_b,\ \dot{\psi}_l,\ \dot{\psi}_t,\ \dot{\psi}_g\right]^T$$

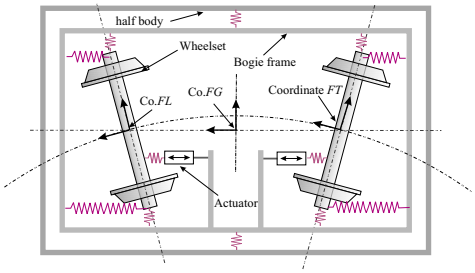


(a) Frames of the vehicle

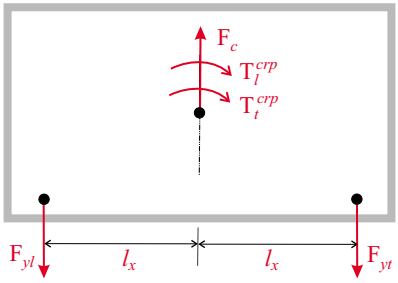


(b) General principles of active steering

Figure 1: A railway vehicle

$$\mathbf{u} = [T_l,\ T_t]^T$$

$$\mathbf{w} = \left[\ \theta_l,\quad \theta_l,\quad \chi_l,\quad \chi_t,\quad \dot{\chi}_l,\quad \dot{\chi}_t,\quad y_{rl},\quad y_{rt}\ \right]^T$$

and the expression of matrices $\mathbf{A}$, $\mathbf{B}$ and $\mathbf{P}$ are given in Appendix A. Generally speaking, the model developed so far, being a linear representation of the system, is suitable for the development of the control strategies, but it is not sufficient for control assessment. A more complicated version [6], including the model of the actuator, the sensor dynamics and the nonlinearities of the wheel conicity, will be applied for evaluating the controllers.

Fig.1 (b) shows a very simple representation of the railway vehicle, being treated as a single rigid body with a mass of $M = 2m_w + m_g + m_b$. In steady-state, only the creep forces $F_{yl}$ and $F_{yt}$ are necessary to counteract the lateral unbalance load (or cant deficiency forces $F_c$) for the vehicle on curves. Thus, the unnecessary creep torques $T_l^{crp}$ and $T_t^{crp}$ can only result from an inappropriate steering. It is clear that in the perfect steering conditions, the following must hold.

$$F_{yl} = F_{yt} = F_c/2 \tag{6}$$

$$T_l^{crp} = T_t^{crp} = 0 \tag{7}$$

in which $F_c = M\ C_d$ and $C_d \approx v_s^2/R - g\ \theta$, where $\theta$ is the cant angle of the track on the curve. Suppose that $y_{rl} = 0$ and $y_{rt} = 0$, the above requirements are equivalent to $\psi_l = \psi_l = \psi_d$ and $y_l = y_t = y_d$, in which $\psi_d$ is the desired angle of attack for both wheelsets while $y_d$ the desired lateral displacement. Referring back to Eqn.(1), (2), (3) and (4), it yields that.

$$\psi_d = -\frac{M\ C_d}{2\ F_{22}} \tag{8}$$

$$y_d = -\frac{l_g\ r_0}{R\ \lambda} \tag{9}$$

Obviously, if the angle of attack and lateral deflections of the wheelsets can be readily measured, it would then be straight forward to design a control for the active steering. Unfortunately these signals are difficult to measure, either expensive sensors are needed or complex estimators have to be used. However, if $\psi_l - \psi_t = 0$ and $y_l - y_t = 0$, the system can meet requirements of the perfect steering. In steady-state, $\psi_l = \psi_t$ implies $F_{yl} = F_{yt}$, leading to $T_l^{crp} + T_t^{crp} = 0$. Likewise, $y_l = y_t$ implies $T_l^{crp} = T_t^{crp}$. Thus $T_l^{crp} = T_t^{crp} = 0$ are the only solution. Noting that $(\psi_l - \psi_g) - (\psi_t - \psi_g)$ is equivalent to $\psi_l - \psi_t$ while $(y_l - y_g) - (y_t - y_g)$ to $y_l - y_t$, it requires only measuring the relative movements of the wheelsets and the bogie.

Although a number of controllers may be developed, this paper proposes a feedforward control law to implement the strategy. The obvious advantage is that it does not interfere with the stability and therefore can be developed independently.

## 3 Feedforward Control Strategies

Radial steering, achieved by passively or actively operating the wheelsets in line with the radius of curvature, generally cannot result in perfect steering except for zero cant deficiency (*i.e.* $C_d = 0$, the centrifugal force is exactly balanced by the gravity force of the vehicle on the canted track). Thus a more sophisticated strategy is necessary. The strategy studied in this paper focuses on the quasi steady-state performance although how to avoid the performance becoming worse during the transition is also under consideration.

The feedforward control laws proposed for the perfect steering are,

$$T_l = K_{pw}^c\left(\psi_d - \frac{l_x}{R^c}\right) \tag{10}$$

$$T_t = K_{pw}^c\left(\psi_d + \frac{l_x}{R^c}\right) \tag{11}$$

in which $\psi_d$ is the desired angle of attack, being given by (8), and $K_{pw}^c$ is the yaw stiffness and $R^c$ is the radius of curvature used in the control law. Perfect steering reduces to radial steering if $\psi_d = 0$. Clearly, the control laws depend on the accuracy of the yaw stiffness $K_{pw}$ and the curvature $R$. Perfect steering is only attained if the parameters are exact.

To prove that above control laws could result in the perfect steering, two new variables are introduced, which are $y^- = y_l - y_t$ and $\psi^- = \psi_l - \psi_t$. Then, the steady-state version of equations of the system becomes

$$F_{22}\psi^- + k_{py}(2l_x\psi_g - y^-) = 0 \tag{12}$$

$$F_{11}\frac{l_g\lambda}{r_0}y^- + K_{pw}\psi^- = L_2 \tag{13}$$

$$l_x k_{py}(2l_x\psi_g - y^-) + 2K_{pw}\psi_g = L_3 \tag{14}$$

in which,

$$L_2 = 2l_x\left(\frac{K_{pw}}{R} - \frac{K_{pw}^c}{R^c}\right)$$

$$L_3 = 2K_{pw}^c\psi_d - K_{pw}(\psi_l + \psi_t)$$

By introducing $\mathbf{L_X} = [y^-, \psi^-, \psi_g]^T$ and $\mathbf{L_Y} = [0, L_1, L_2]^T$, then

$$\mathbf{L_Y} = \mathbf{L_A}\ \mathbf{L_X}$$

where

$$\mathbf{L_A} = \begin{bmatrix} -k_{py} & F_{22} & 2l_x k_{py} \\ F_{11}\frac{l_g\lambda}{r_0} & K_{pw} & 0 \\ -l_x k_{py} & 0 & 2K_{pg} \end{bmatrix}$$

It is true in this case that the singular values of $\mathbf{L_A}$ all exist and positive, thus

$$\frac{\|\mathbf{L_Y}\|_2}{\overline{\sigma}(\mathbf{L_A})} \le \|\mathbf{L_X}\|_2 \le \frac{\|\mathbf{L_Y}\|_2}{\underline{\sigma}(\mathbf{L_A})}$$

The perfect feedforward control law (10) and (11) with precise knowledge of yaw stiffness and curvature results in $L_2 = 0$ and $L_3 = 0$ (since $2\psi_d = \psi_l + \psi_t$ ), therefore $y^- = 0$, $\psi^- = 0$ and $\psi_g = 0$ are unique solution of the system, implying the perfect steering conditions of $y_l = y_t = y_d$ and $\psi_l = \psi_l = \psi_d$. Excluding $\psi_d$ from the control law leads to $L_3 = -2K_{px}\psi_d$, which in turn results in $y^-$, $\psi^-$ and $\psi_g$ being not equal to zero. This confirms that radial steering is not perfect, and the distance from the ideal depends on the size of $\psi_d$ since $\|\mathbf{L_Y}\|_2 = 2K_{pw}\psi_d$ (finally on the magnitude of $C_d$). On the other hand, the performance of the proposed control law is affected by parameter variations such as the inaccuracies of the curvature $\Delta R$ and the yaw stiffness $\Delta K_{pw}$. The $\Delta R$ (*i.e.* $R^c = R + \Delta R$) leads to $L_2 = 2l_x\Delta R/R^2$. Thus,

$$\frac{2l_x\Delta R}{R^2\ \overline{\sigma}(\mathbf{L_A})} \le \|\mathbf{L_X}\|_2 \le \frac{2l_x\Delta R}{R^2\ \underline{\sigma}(\mathbf{L_A})}$$

it is clear that the system performance depends both on the

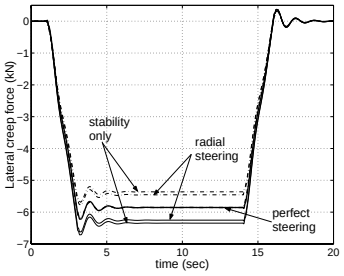


(a) Lateral forces

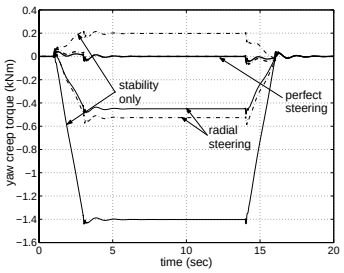


(b) yaw torques

Figure 2: Creep forces

curvature variation and the curvature itself. Moreover, the variations of yaw stiffness $\Delta K_{pw}$ (*i.e.* $K^c_{pw} = K_{pw} + \Delta K_{pw}$) yields $L_2 = 2\Delta K_{pw} l_x/R$ and $L_3 = 2\Delta K_{pw}\psi_d$. Then, the inequation given below reveals how $\Delta K_{pw}$ affects the steering.

$$\frac{2\Delta K_{pw}\sqrt{R^2\psi_d^2 + l_x^2}}{R\ \overline{\sigma}(\mathbf{L_A})} \le \|\mathbf{L_X}\|_2 \le \frac{2\Delta K_{pw}\sqrt{R^2\psi_d^2 + l_x^2}}{R\ \underline{\sigma}(\mathbf{L_A})}$$

Equation (12) implies that only two of $y^-$, $\psi^-$, and $\psi_g$ are independent, indicating the idea of $y_l = y_t$ and $\psi_l = \psi_t$ is sufficient to achieve the perfect steering. The equal lateral forces (*i.e.* $\psi_l = \psi_t$) alone however does not necessarily lead to zero longitudinal creep as $\psi^- = 0$ can also give $y^- = 2l_x\psi_g$.

## 4 Simulation and analysis

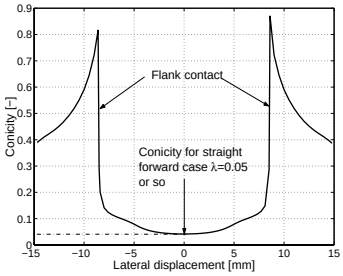


(a) Nonlinearity of the conicity

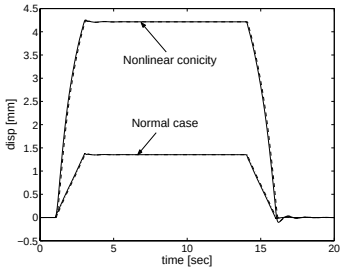


(b) Lateral displacements

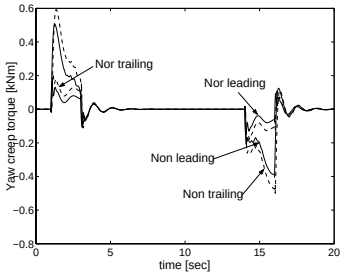


(c) Yaw creep torques

Figure 3: Results for the nonlinearity

Computer simulations are used to compare the performance of the different strategies, which are the stability control only, the radial and the perfect steering.

Fig.2 shows that the perfect feedforward strategy yields equal lateral and zero longitudinal creep forces in quasi steady-state whereas the radial steering and the stability control only strategy do not. If the lateral creepages of the leading (solid-line) and trailing (dash-line) wheelset are unequal, the yaw creep torques at leading and trailing wheelsets are essential to balance the torque they generated. The stability control only strategy is the worst. Clearly, none of them can reach perfect steering dur-

ing transients and it takes 2 $sec$ or so for the system to settle down.

One of the objectives of this paper is to assess the performance of the control laws in different conditions including vehicle speed change and system uncertainties. A number of indices, are introduced for the assessment. $\mathcal{T}_l$ and $\mathcal{T}_t$, which are root mean square (*r.m.s*) of $T_l$ and $T_t$ respectively, are applied to evaluate the magnitude of the control effort. Likewise, $\mathcal{F}_{yl}$ and $\mathcal{F}_{yt}$ are utilized as indicators for lateral creep forces of individual wheelset.

$$\mathcal{F}_{yl} = \frac{T_c\sqrt{\frac{1}{T_s}\int_0^{T_s}[F_{yl}(t)-F_d(t)]^2dt}}{T_s\ \sup_{t\in[0,T_s]}|F_d(t)|}$$

where $T_s$ is the duration of assessment, $T_c$ the period on

Table 1: Uncertainties for assessment($v_s = 50\ m/s$,)

| Title | Name | Content |
|---|---|---|
| $Nor$ | Normal case | $\lambda = 0.2$,$C_d = 1$ |
| $Cef$ | Creep coefficients | $f_{11}$,$f_{22}$ decreases 20% |
| $Yws$ | Yaw stiffness | Increases 20% |
| $Sts$ | Steering link. stiffness | Increases 80% |
| $Non$ | Conicity nonlinearity | Includes |

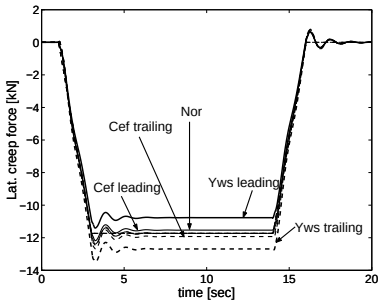


(a) Lateral creep forces

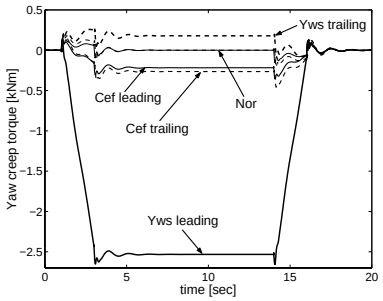


(b) Yaw creep torques

Figure 4: Results for parameter uncertainties

curves, $F_d$ is the desired creep force at individual wheelsets which has the value of $F_c/2$. The expression for $\mathcal{F}_{yt}$ is the same as that of $\mathcal{F}_{yl}$ except substituting $F_{yl}$ by $F_{yt}$. The longitudinal forces are standardised as $\mathcal{F}_{xl}$ and $\mathcal{F}_{xt}$, only the expression of $\mathcal{F}_{xl}$ being given.

$$\mathcal{F}_{xl} = \frac{T_c\sqrt{\frac{1}{T_s}\int_0^{T_s}\left(\frac{T_l^{crp}}{l_g}\right)^2dt}}{T_s\ \sup_{t\in[0,T_s]}|F_d(t)|}$$

Furthermore, $\mathcal{W}_l$ and $\mathcal{W}_t$ are employed as wear indices of the

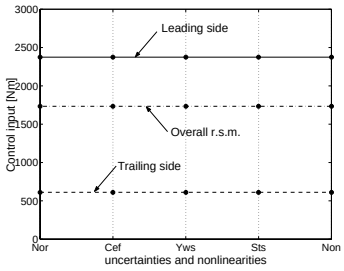


(a) Control inputs

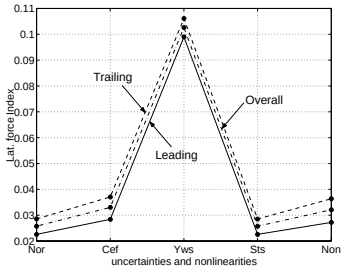


(b) Lateral forces

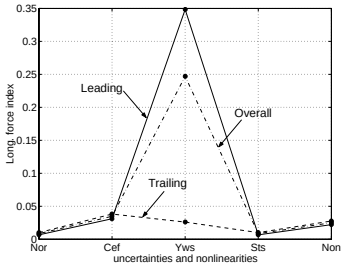


(c) Longitudinal forces

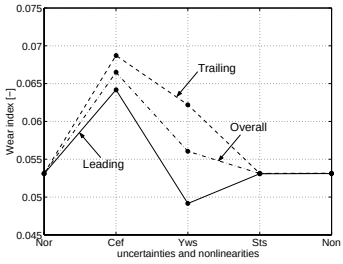


(d) Wear

Figure 5: Results for different cant deficiencies ($\lambda = 0.3$)

wheelsets, being *r.m.s* of $W_l$ and $W_t$ [8].

$$W = \begin{cases} 0.005 \times C_{rep} \times F_{sum} & C_{rep}F_{sum} \leq 160 \\ 0.025 \times C_{rep} \times F_{sum} - 3.2 & C_{rep}F_{sum} > 160 \end{cases}$$

in which $C_{rep}$ and $F_{sum}$ are magnitudes of total creepage and creep force. $\mathcal{T}$ is used to evaluate the overall size of control inputs, being give by.

$$\mathcal{T} = \sqrt{\frac{\mathcal{T}_l^2 + \mathcal{T}_t^2}{2}}$$

Similarly, $\mathcal{F}_y$, $\mathcal{F}_x$ and $\mathcal{W}$ are for the overall lateral and longitudinal forces, and wheelset wear.

The control design is based on the knowledge of parameters, however the precise knowledge is not always possible. It is, therefore, necessary to evaluate the sensitivities of the control laws under the parameter variations and the nonlinearity of the conicity. Table.4 lists all the cases to be assessed, and Fig.3 (a) presents the nonlinearity of the wheel conicity used in the study.

A comparison of the results between linear and nonlinear concities is given in Fig.3 (b) and (c), in which only the lateral displacements and the yaw torques due to the longitudinal creep forces are presented. The nonlinearity plays a key role on the quasi steady-state lateral displacement, since on some curves the conicity of the wheel at the contact point with rail is much less than the magnitude of $0.2$ used in norminal case. As a consequence, it results in a larger displacement causing a worse transient longitudinal forces as shown in figure (c). Nevertheless, the nonlinearity does not affect the steady-state steering of the vehicle. Fig.4 shows the results for the parameter uncertainties of the creep coefficients and the yaw stiffness. In either case, the perfect steering is not achieved as expected. In particular, the performance due to the yaw stiffness variation is much worse than that to the coefficient variation. Therefore though the creep coefficients play a part, the yaw stiffness is more critical for the perfect steering control law.

Figure 5(d) shows that the variation of the creep coefficients contribute most to the wear of the wheelsets, however the variation of the yaw stiffness produce the most uneven wear among the wheelsets. The indices given in 5 (b) and (c) discover the relative distances of the creep forces from the their desire values, providing another way to evaluate the 'How bad or good' of a steering. The relative distance of lateral forces from perfect steering with $20\%$ yaw stiffness uncertainty is about $10\%$. On the contrary, there figures for the coefficient and nonlinearity are around $3\%$, being very close to 2.5 percent for the normal case. Moreover, the relative distance of the longitudinal forces of yaw stiffness uncertainty is much worse. All the indices for $80\%$ steering linkage steering increase are almost same with those of the normal case, proving the system insensitivity toward it. Not surprisingly, The control effort remains same for the various parameter variations (as shown in Fig.5(a)). This explains the control law has no react to parameter variations.

## 5 Conclusions

Unlike the radial and stability control only strategy, the proposed feedforward strategy has the capability of achieving the perfect performance without interference of the vehicle stability. This strategy requires the knowledge of the designed angle of attach depending on the cant deficiency, the mass of the vehicle, the creep coefficients. In addition, the sensitivity to parameter variations are analysed and verified by the simulations. Among the others, the yaw stiffness variation is most significant one. It is, therefore significant to improve the system performance under the yaw stiffness variation. Incorporation with some feedback strategies can overcome this problem but request further investigation.

## References


[1] Wickens, A.H.: Stability Criteria for Artculated Railway Vehicles Possessing Perfecting Steering. *Vehicle System Dynamics* 7 (1978), pp. 165–182.

[2] Shen, G., Goodall, R.M.: Active Yaw Relaxation for Improved Bogie Performance. *Vehicle System Dynamics* 28 (1997), pp. 273–282.

[3] Illingworth, R. and Pollard, M.G.: The Use of Steering Acitve Suspension to Reduce Wheel and Rail Wear in Curves. *Proc. Instn. Mech. Engrs* 196 (1982), pp. 379–385.

[4] Mei, T.X. and Goodall, R.M.: Modal Controllers for Active Steering of Railway Vehicles with Solid Axle wheelsets. *Vehicle System Dynamics* 34 (2000), pp. 24–31.

[5] Perez, J., Busturia, J.M., Goodall, R.M.,: Control strategies for active steering of bogie-based railway vehicles. *Control Engineering Pratice* 10 (2002), pp. 1005–1012.

[6] Mei, T.X. and Goodall, R.M.: Robust Control of Independently Rotating Wheelsets on a Railway Vehicle Using Practical Sensors. *IEEE Trans. on Control System Technology* 9 (2001), pp. 599–607.

[7] Goodall, R.M., Li, H.: Solid Axle and Independenly-Rotating Railway Wheelsets - A Control Engineering Assessment of Stability. *Vehicle System Dynamics* 33 (2000), pp. 57–67.

[8] Mei, T.X. and Goodall, R.M.: A comparison of control strategies for active steering of railway wheelsets. *AVEC 2000*, Ann Arbor, Michigan, 2000.


## A Matrices A, B, and P

$$\mathbf{A} = \begin{bmatrix} \mathbf{O}_{7\times7} & \mathbf{I}_{7\times7} \\ \mathbf{A}_{21} & \mathbf{A}_{22} \end{bmatrix} \qquad \mathbf{B} = \begin{bmatrix} \mathbf{O}_{7\times2} \\ \mathbf{B}_2 \end{bmatrix} \qquad \mathbf{P} = \begin{bmatrix} \mathbf{O}_{7\times8} \\ \mathbf{P}_2 \end{bmatrix}$$

in which, $\mathbf{I}$ represents the identical matrix while $\mathbf{O}$ corresponds to the zero matrix.

$$\mathbf{A}_{21} = \begin{bmatrix} \frac{-k_{py}}{m_w} & 0 & \frac{k_{py}}{m_w} & 0 & \frac{F_{22}}{m_w} & 0 & \frac{k_{py}l_x}{m_w} \\ 0 & \frac{-k_{py}}{m_w} & \frac{k_{py}}{m_w} & 0 & 0 & \frac{F_{22}}{m_w} & \frac{-k_{py}l_x}{m_w} \\ \frac{k_{py}}{m_g} & \frac{k_{py}}{m_g} & \frac{-2k_{py}-k_y}{m_g} & \frac{k_y}{m_g} & 0 & 0 & 0 \\ 0 & 0 & \frac{k_y}{m_b} & \frac{-k_y}{m_b} & 0 & 0 & 0 \\ \frac{-l_g F_{11}\lambda}{r_0 I_w} & 0 & 0 & 0 & \frac{-K_{pw}}{I_w} & 0 & \frac{K_{pw}}{I_w} \\ 0 & \frac{-l_g F_{11}\lambda}{r_0 I_w} & 0 & 0 & 0 & \frac{-K_{pw}}{I_w} & \frac{K_{pw}}{I_w} \\ \frac{l_x k_{py}}{I_g} & \frac{-l_x k_{py}}{I_g} & 0 & 0 & \frac{K_{pw}}{I_g} & \frac{K_{pw}}{I_g} & \frac{-2K_{pg}}{I_g} \end{bmatrix}$$

$$\mathbf{A}_{22} = \begin{bmatrix} \frac{\frac{-F_{22}}{v_s}-b_{py}}{m_w} & 0 & \frac{b_{py}}{m_w} & 0 & 0 & 0 & \frac{b_{py}\,l_x}{m_w} \\ 0 & \frac{\frac{-F_{22}}{v_s}-b_{py}}{m_w} & \frac{b_{py}}{m_w} & 0 & 0 & 0 & \frac{-b_{py}l_x}{m_w} \\ \frac{b_{py}}{m_g} & \frac{b_{py}}{m_g} & \frac{-2b_{py}-b_y}{m_g} & \frac{b_y}{m_g} & 0 & 0 & 0 \\ 0 & 0 & \frac{k_y}{m_b} & \frac{k_y}{m_b} & 0 & 0 & 0 \\ 0 & 0 & 0 & 0 & \frac{\frac{-F_{11}l_g^2}{v_s}-B_{pw}}{I_w} & 0 & \frac{B_{pw}}{I_w} \\ 0 & 0 & 0 & 0 & 0 & \frac{\frac{-F_{11}l_g^2}{v_s}-B_{pw}}{I_w} & \frac{B_{pw}}{I_w} \\ \frac{l_x b_{py}}{I_g} & \frac{-l_x b_{py}}{I_g} & 0 & 0 & \frac{B_{pw}}{I_g} & \frac{B_{pw}}{I_g} & \frac{-2B_{pg}}{I_g} \end{bmatrix}$$

$$\mathbf{B}_2 = \begin{bmatrix} 0 & 0 \\ 0 & 0 \\ 0 & 0 \\ 0 & 0 \\ \frac{1}{I_w} & 0 \\ 0 & \frac{1}{I_w} \\ \frac{-1}{I_g} & \frac{-1}{I_g} \end{bmatrix}$$

$$\mathbf{P}_2 = \begin{bmatrix} -g & 0 & v_s^2 & 0 & 0 & 0 & 0 & 0 \\ 0 & -g & 0 & v_s^2 & 0 & 0 & 0 & 0 \\ \frac{-g}{2} & \frac{-g}{2} & \frac{v_s^2}{2} & \frac{v_s^2}{2} & 0 & 0 & 0 & 0 \\ \frac{-g}{2} & \frac{-g}{2} & \frac{v_s^2}{2} & \frac{v_s^2}{2} & 0 & 0 & 0 & 0 \\ 0 & 0 & \frac{F_{11} l_g^2 + K_{pw} l_x}{I_w} & 0 & v_s + \frac{B_{pw} l_x}{I_w} & 0 & \frac{l_g F_{11} \lambda}{r_0 I_w} & 0 \\ 0 & 0 & 0 & \frac{F_{11} l_g^2 - K_{pw} l_x}{I_w} & 0 & v_s - \frac{B_{pw} l_x}{I_w} & 0 & \frac{l_g F_{11} \lambda}{r_0 I_w} \\ 0 & 0 & \frac{-K_{pw} l_x}{I_g} & \frac{K_{pw} l_x}{I_g} & \frac{v_s}{2} - \frac{B_{pw} l_x}{I_g} & \frac{v_s}{2} + \frac{B_{pw} l_x}{I_g} & 0 & 0 \end{bmatrix}$$

# B Nomenclature

$b_{px}$, $b_{py}$ : longitudinal, lateral damping per wheelset of primary suspensions
$b_y$ : lateral damping per bogie of secondary suspensions
$B_{pw}$, $B_{pg}$ : equivalent yaw damping of primary suspensions per wheelset, bogie
$C_d$ : cant deficiency,
$f_{11}$, $f_{22}$ : longitudinal, lateral creep coefficient
$F_{yl}$, $F_{yt}$ : lateral creep force at leading, trailing wheelset
$g$ : gravity
$I_w$, $I_g$ : wheelset, bogie yaw inertia,
$k_{px}$, $k_{py}$ : longitudinal, lateral stiffness per wheelset of primary suspensions
$k_y$ : lateral stiffness per bogie of secondary suspensions
$K_{pw}$, $K_{pg}$ : equivalent yaw stiffness of primary suspensions per wheelset, bogie
$l_y$ : half spacing of longitudinal primary suspension,
$l_x$ : half longitudinal spacing of wheelsets,
$l_g$ : half gauge of wheelset
$m_w$, $m_g$, $m_b$ : wheelset, bogie, half body mass
$r_0$ : wheel radius
$R$ : radius of the curved track
$R_l$, $R_t$ : radius of the curved track at leading, trailing wheelset
$T_l$, $T_t$ : active control torque input at leading, trailing wheelset
$T_l^{crp}$, $T_t^{crp}$ : creep torque at leading, trailing wheelset
$v_s$ : vehicle forward speed
$y_l$, $y_t$ : lateral displacement of leading wheelset, *w.r.t.* frame $FL$
$y_t$ : lateral displacement of trailing wheelset, *w.r.t.* frame $FT$
$y_g$, $y_b$ : lateral displacement of the bogie, half body *w.r.t.* frame $FG$
$y_{rl}$, $y_{rt}$ : track lateral irregularity of leading wheelset,
$\lambda$ : wheel conicity,
$\psi_l$ : yaw angle of leading wheelset, *w.r.t.* frame $FL$
$\psi_t$ : yaw angle of trailing wheelset, *w.r.t.* frame $FT$
$\psi_g$ : yaw angle of the bogie, *w.r.t.* frame $FG$
$\theta$ : track cant angle
$\theta_l$, $\theta_t$ : track cant angle on curves track at leading, trailing wheelset

# C Nominal Parameters

| | | | | | |
|---|---|---|---|---|---|
| $b_{px}$ | 1.2e4 | Ns/m | $b_{py}$ | 2.4e4 | Ns/m |
| $b_y$ | 4.0e4 | Ns/m | $f_{11}$ | 1e7 | N |
| $f_{22}$ | 1e7 | N | $I_w$ | 766 | kg/m$^2$ |
| $I_g$ | 3200 | kg/m$^2$ | $k_{px}$ | 1.9e6 | N/m |
| $k_{py}$ | 9.4e6 | N/m | $k_{py}$ | 4.9e5 | N/m |
| $l_x$ | 1.225 | m | $l_y$ | 1.0 | m |
| $l_g$ | 0.75 | m | $m_w$ | 1376 | kg |
| $m_g$ | 3477 | kg | $m_b$ | 17230 | kg |
| $r_0$ | 0.445 | m | $v_s$ | 65 | m/s |
| $\lambda$ | 0.3 | - | $\theta$ | 0.1047 | rad |